

RESEARCH ARTICLE

 OPEN ACCESS

## Chrysofenetin inhibits artemisinin efflux in P-gp-over-expressing Caco-2 cells and reverses P-gp/MDR1 mRNA up-regulated expression induced by artemisinin in mouse small intestine

Liping Ma<sup>a\*</sup>, Shijie Wei<sup>b\*</sup>, Bei Yang<sup>a</sup>, Wei Ma<sup>a</sup>, Xiuli Wu<sup>a</sup>, Hongyan Ji<sup>b</sup>, Hong Sui<sup>a</sup> and Jing Chen<sup>a</sup>

<sup>a</sup>School of Pharmacy, Ningxia Medical University, Yinchuan, Ningxia, PR China; <sup>b</sup>Institute of Clinical Pharmacology, General Hospital of Ningxia Medical University, Yinchuan, Ningxia, PR China

### ABSTRACT

**Context:** CYP3A4 and P-gp together form a highly efficient barrier for orally absorbed drugs and always share the same substrates. Our previous work revealed that chrysofenetin (CHR) significantly augmented the rat plasma level and anti-malarial efficacy of artemisinin (ART), partially due to the uncompetitive inhibition effect of CHR on rat CYP3A. But the impact of CHR on P-gp is still unknown.

**Objective:** The present study investigates whether CHR interferes with P-gp-mediated efflux of ART and elucidates the underlying mechanism.

**Materials and methods:** P-gp-over-expressing Caco-2 cells were treated with ART (10  $\mu$ M) or ART-CHR (1:2, 10:20  $\mu$ M) in ART bidirectional transport experiment. ART concentration was determined by UHPLC-MS/MS method. Healthy male ICR mice were randomly divided into nine groups ( $n=6$ ) including negative control (0.5% CMC-Na solution, 13 mL/kg), ART alone (40 mg/kg), verapamil (positive control, 40 mg/kg), ART-verapamil (1:1, 40:40 mg/kg), CHR alone (80 mg/kg), ART-CHR (1:0.1, 40:4 mg/kg), ART-CHR (1:1, 40:40 mg/kg), ART-CHR (1:2, 40:80 mg/kg) and ART-CHR (1:4, 40:160 mg/kg). The drugs were administrated intragastrically for seven consecutive days. MDR1 and P-gp expression levels in mice small intestine were examined by performing RT-PCR and western blot analysis. ABC coupling ATPase activity was also determined.

**Results:** After combined with CHR (1:2),  $P_{app}$  (AP-BL) and  $P_{app}$  (BL-AP) of ART changed to  $4.29 \times 10^{-8}$  (increased 1.79-fold) and  $2.85 \times 10^{-8}$  cm/s (decreased 1.24-fold) from  $2.40 \times 10^{-8}$  and  $3.54 \times 10^{-8}$  cm/s, respectively. Efflux ratio ( $P_{BA}/P_{AB}$ ) declined 2.21-fold ( $p < 0.01$ ) versus to ART alone. ART significantly up-regulated both MDR1 mRNA and P-gp levels compared with vehicle, while CHR in combination ratio of 0:1, 0.1:1, 1:1, 2:1 and 4:1 with ART, reversed them to normal levels as well as negative control ( $p < 0.05$ ). The ATPase activities in ART-CHR 1:4 and CHR alone groups achieved a slight increase ( $p < 0.05$ ) when compared with ART alone.

**Discussion and conclusion:** These results confirm that CHR inhibited P-gp activity and reverse the up-regulated P-gp and MDR1 levels induced by ART. It suggested that CHR potentially can be used as a P-gp reversal agent to obstruct ART multidrug resistance.

### ARTICLE HISTORY

Received 23 March 2016  
Revised 24 July 2016  
Accepted 23 September 2016

### KEYWORDS



Polymethoxylated flavonoids; antimalarial drugs; ABC transporters; P-glycoprotein

### Introduction

To date, artemisinin (ART, [Figure 1\(A\)](#)) antimalarial drugs are still of the utmost importance in the worldwide combination therapy of resistant *Plasmodium falciparum* (Tripathi et al. 2013). Unfortunately, ART resistance defined as a delayed clearance of parasites after clinical therapy has been reported (Meshnick et al. 1996; White 2004). The mechanism of ART resistance, however, is nearly unknown and probably modulated by multiple mechanisms, which mainly involved multidrug resistance proteins such as several members of the ATP-binding cassette (ABC) transporter super-family (Burk et al. 2005; Alcantara et al. 2013). Among them, P-gp (MDR1) is the most extensively studied efflux transporter responsible for limiting the intestinal absorption of a diverse range of xenobiotics. P-gp usually shares the identical substrates with human CYP3A4/rat CYP3A (Pal et al. 2011;

Nabekura et al. 2015; Wang et al. 2015). This causes the low bio-availability and blood concentration for terminal drugs (Meng et al. 2014). Burk et al. (2005) suggested that ART induced the expression of CYP2B6, CYP3A4 and MDR1 through activating human PXR as well as human and mouse CAR as a ligand of both two nuclear receptors.

Many polymethoxylated flavonoids are able to modulate the activity of drug-metabolizing enzymes and ABC transporters, which raises the potential for alterations in the pharmacokinetics of substrate drugs (Li et al. 2010; Wesolowska 2011; Yuan et al. 2012). Chrysofenetin (CHR, [Figure 1\(B\)](#)) is one of the polymethoxylated flavonoids in *Artemisia annua* L. (Compositae) and other several Chinese herbs (Numonov et al. 2015). In our previous study (Chen et al. 2014), CHR was observed to be abundant in the acetone layer, among which of the five parts of waste materials (petroleum ether layer, petroleum ether-acetate ethyl layer,

**CONTACT** Prof. Jing Chen  chenjing2005@126.com  School of Pharmacy, Ningxia Medical University, No.1160 Shengli Street, Xingqing District, Yinchuan, Ningxia 750004, PR China

\*These authors contributed equally to this work.

© 2016 The Author(s). Published by Informa UK Limited, trading as Taylor & Francis Group.

This is an Open Access article distributed under the terms of the Creative Commons Attribution License (<http://creativecommons.org/licenses/by/4.0/>), which permits unrestricted use, distribution, and reproduction in any medium, provided the original work is properly cited.

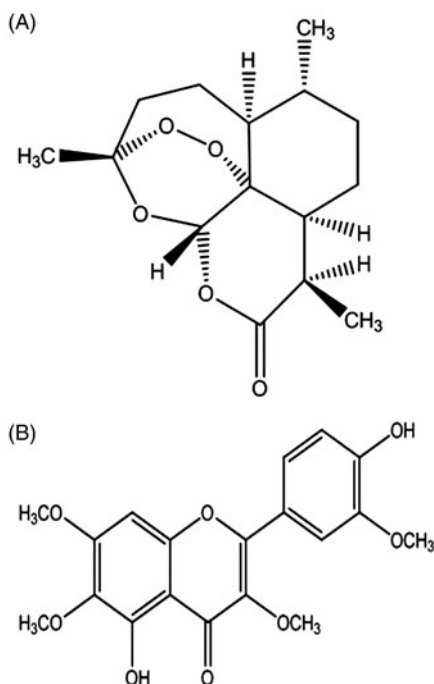


Figure 1. Structures of ART (A) and chryso splenetin (B).

ethanol layer, acetone layer and the residues after extraction) produced during ART industrial purification from leaves of *A. annua*. A patent for the purification of CHR from the acetone layer was granted in 2014 (Chen et al. 2014). Furthermore, CHR significantly increased rat plasma concentration of ART and its anti-malarial efficacy, partially due to the inhibition effect of CHR on rat CYP3A in an uncompetitive manner (Wei et al. 2015).

In the present research, we further confirmed the inhibition of CHR on P-gp-mediated efflux of ART in P-gp-over-expressing Caco-2 cells and the reversal of CHR on the up-regulated MDR1 and P-gp levels induced by ART in small intestine of mice. Our study provides a better understanding of CHR function as a potent small molecular inhibitor on P-gp-mediated ART multi-drug resistance.

## Materials and methods

### Animals

Healthy male ICR mice (18–22 g of body weight) were purchased from SPF Animal Centre of Ningxia Medical University (Ningxia, China). The permission number was SCXK 2010-0002. All animals were housed in polycarbonate cages and acclimated in an environmentally controlled room ( $23 \pm 2^\circ\text{C}$ , with adequate ventilation and a 12 h light/dark cycle) prior to use. All animals were provided with standard laboratory food and water before and during the experiments. The experimental protocol was approved by the University Ethics Committee. All procedures involving animals were in accordance with the Regulations of the Experimental Animal Administration, State Committee of Science and Technology. Animals were randomly divided into nine groups ( $n=6$  for each group) including negative control (0.5% CMC-Na solution, 13 mL/kg), ART alone (40 mg/kg), verapamil (positive control, 40 mg/kg), ART-verapamil (1:1, 40:40 mg/kg), CHR alone (80 mg/kg), ART-CHR (1:0.1, 40:4 mg/kg), ART-CHR (1:1, 40:40 mg/kg), ART-CHR (1:2, 40:80 mg/kg) and ART-CHR (1:4, 40:160 mg/kg). The drugs were administered intragastrically for seven consecutive days.

### Materials and instruments

Verapamil hydrochloride tablets (No.140101) were purchased from Guangdong Hua-nan Pharmaceutical Group Co., Ltd (Guangdong China). ART (white crystal, purity >99.0%, Chongqing, China) was purchased from Chongqing Huali Konggu Co., Ltd. (Beijing, China). CHR (yellow crystal, purity >98.0%) was purified in our lab from an acetone layer of ART industrial waste materials using multiple column chromatography methods with yield around 1% according to our patent (Chen et al. 2014). The industrial wastes were kindly provided by Chongqing Huali Konggu Co., Ltd and the voucher specimen has been deposited with College of Pharmacy, Ningxia Medical University, for further references.

### Bidirectional transport experiments in P-gp-over-expressing Caco-2 cell monolayers

Cells were seeded in the transwell polycarbonate inserts at a density of  $10^6$  cells per well and were grown in a culture medium consisting of Dulbecco's modified eagle's medium supplemented with 10% foetal bovine serum, 1% non-essential amino acids, 1% L-glutamine, 100 U/mL penicillin-G and 100  $\mu\text{g}/\text{mL}$  streptomycin. The culture medium was replaced every alternate day and the cells were maintained at  $37^\circ\text{C}$ , 95% relative humidity and 5%  $\text{CO}_2$ . Permeability studies were conducted with the monolayers cultured for 19–21 d. Monolayers with transepithelial electrical resistance (TEER) values higher than  $420 \Omega/\text{cm}^2$  were used for the experiments. Before the experiments, cell monolayers were washed twice with warm HBSS and equilibrated with HBSS for 30 min at  $37^\circ\text{C}$ . HBSS containing ART (10  $\mu\text{M}$ ) or ART-CHR (1:2, 10:20  $\mu\text{M}$ ) was added to either the apical or basolateral chamber (donor chamber), and blank HBSS was added to the opposite chamber (receiver chamber). The total volume is 2.5 mL in apical chamber and 2.5 mL in the basolateral chamber. A 200  $\mu\text{L}$  aliquot of samples was separately taken from the donor and receiver chambers each 1 h until 6 h and the same volume (200  $\mu\text{L}$ ) of blank HBSS was immediately added, respectively. Transport experiments were conducted in an incubator maintained at  $37^\circ\text{C}$  and shaken with a speed of 50 rpm. The samples were dried in  $\text{N}_2$  and the residues were resolved by 50% methanol under a 30 s vortex. About 20  $\mu\text{L}$  of blank HBSS and 200  $\mu\text{L}$  of IS (daidzein, 0.5  $\mu\text{M}$ ) were added into 20  $\mu\text{L}$  of samples. After a 30 s vortex, the mixture was centrifuged at 10,000 rpm and  $4^\circ\text{C}$  for 10 min. The concentration of ART was determined by UHPLC-MS/MS.

$P_{\text{app}}$  values across the cell monolayers were calculated according to the equation:

$$P_{\text{app}}(\text{cm/s}) = \frac{dQ}{dt} \times \frac{1}{A \times C_0},$$

where  $dQ/dt$  represents the rate of drug transport.  $A$  is the surface area of the cell monolayer ( $4.2 \text{ cm}^2$ ).  $C_0$  is the initial concentration of ART in the donor chamber. Efflux ratio was calculated by dividing  $P_{\text{app}}$  (BL-AP) by  $P_{\text{app}}$  (AP-BL).  $P_{\text{app}}$  (AP-BL) represents the transport of ART from the apical to basal side and  $P_{\text{app}}$  (BL-AP) represents that from the basal to apical side.

### Determination of ART using UHPLC-MS/MS method

The UHPLC conditions were as follows: Waters Acquity<sup>TM</sup> with diode array detector (DAD); column, Acquity UHPLC BEH C<sub>18</sub> column (50 mm  $\times$  2.1 mm I.D., 1.7  $\mu\text{m}$ , Waters, Milford, MA);

mobile phase A (0.1% formic acid in water); mobile phase B (acetonitrile); gradient, 0–0.5 min, 95% B; 0.5–2.0 min, 95–40% B; 2.0–4.0 min, 40–90% B; 4–4.5 min, 90–5% B; 4.5–5 min, 95% B; column temperature, 45 °C; sample temperature, 20 °C; and injection volume, 10  $\mu$ L (Sun et al. 2015).

The MS analysis was performed on an API 5500 Qtrap triple quadrupole mass spectrometer (Applied Biosystem/MDS SCIEX, Foster City, CA) equipped with TurboIon Spray<sup>TM</sup> source. The compounds were determined by using multiple reaction monitoring (MRM) scan type in positive mode. The instrument-dependent parameters for mass spectrum were set as follows: ion-spray voltage, 5.5 kV; ion source temperature, 400 °C; nebulizer gas (gas 1), nitrogen, 40 psi; turbo gas (gas 2), nitrogen 20 psi; curtain gas, nitrogen 20 psi. The collision energy was 20 eV for ART and 32 eV for IS. Base on the full-scan mass spectra of each analyte, the MRM transition  $m/z$  283  $\rightarrow$  151 (Figure 2(A) and (B)) for ART was selected for quantitative analysis of ART and  $m/z$  225  $\rightarrow$  199 for daidzein (Figure 2(C) and (D)).

### RNA extraction and quantitative polymerase chain reaction (qPCR)

The mice were euthanized by cervical vertebra dislocation. Small intestines were harvested and cleaned using normal saline at least three times. Total RNA was extracted from the mouse small intestine using E.Z.N.A.<sup>TM</sup> Total RNA Kit (OMEGA Bio-Tek, Norcross, GA), in accordance with the instructions of the manufacturer. RNA concentrations were measured with a microplate spectrophotometer (Bio-RAD, Hercules, CA) at 260 nm. RNA quality was evaluated using electrophoresis in 1% agarose gels.

Total RNA (3  $\mu$ g) was reverse transcribed into first-strand complementary DNA (cDNA) using Thermo Scientific RevertAid First Strand cDNA Synthesis Kit (Thermo Scientific, Waltham, MA). Each cDNA sample (1  $\mu$ L) was amplified with 12  $\mu$ L Thermo Scientific Maxima SYBR Green qPCR Master Mix (2 $\times$ ). ROX Solution provided (Thermo Scientific, Waltham, MA) and 1  $\mu$ mol of each primer. Amplification was performed in a Real Time PCR IQ5 System (Applied Biosystems, Foster City, CA) with the following parameters: denaturation at 94 °C for 2 min followed by 35 cycles of denaturation at 94 °C for 30 s, annealing at 61 °C for 30 s and extension at 72 °C for 45 s. The sequences of the oligonucleotide primers used for this study were 5'-GGG CAC AAA CCA GAC AAC AT-3' (sense) and 5'-TCC GCT CTT CAC CTT CAG AT-3' (antisense) for MDR1 (product size, 117 bp from Sangon Biotech (Shanghai) Co., Ltd., Shanghai, Japan); and 5'-GGT GAA GGT CGG TGT GAA CG-3' (sense) and 5'-CTC GCT CCT GGA AGA TGG TG-3' (antisense) for GAPDH (product size, 233 bp, from Invitrogen Biotechnology Co., Ltd, Carlsbad, CA). The relative expression levels of MDR1 in each sample (normalized to that of GAPDH) were determined using 2<sup>- $\Delta\Delta C_t$</sup>  method (Inami et al. 2015; Zhang et al. 2015; Hao et al. 2016). All qPCR experiments were repeated three times.

### Determination of the expression levels of P-gp by western blot analysis

Membrane proteins were harvested by KenGEN Membrane and Plasma Protein Purification Kit (KenGEN BioTECH, Nanjing, China), and the protein concentrations were determined using KeyGEN BCA Protein Quantitation Assay kit (KenGEN

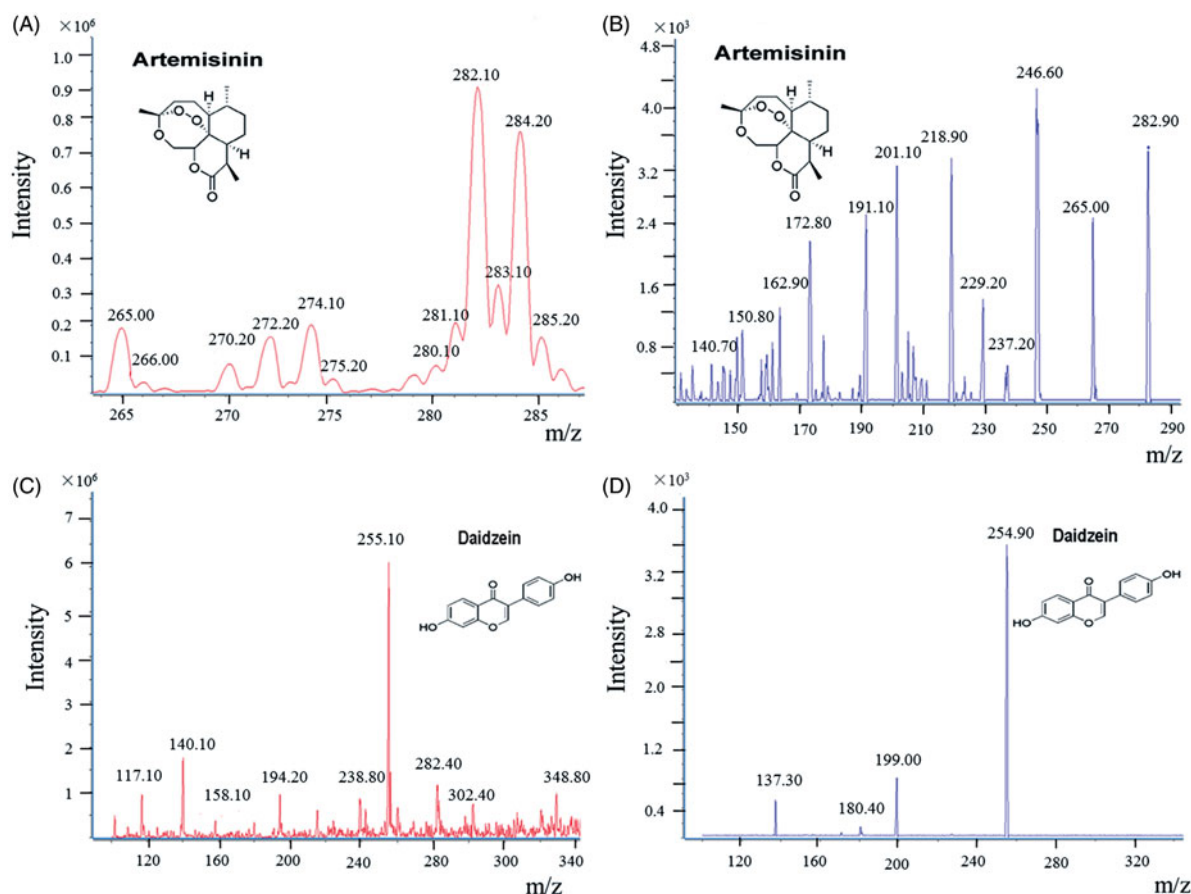


Figure 2. Collision-induced dissociation mass spectra for ART (A: MS<sup>1</sup> and B: MS<sup>2</sup>) and daidzein (C: MS<sup>1</sup> and D: MS<sup>2</sup>).

BioTECH, Nanjing, China). An equal quantity of protein (48 µg) from membrane protein was resolved using 7.5% SDS-PAGE gel and subsequently transferred onto nitrocellulose membranes (Bio-Trace, Auckland, New Zealand). After blocking the membrane with 5% non-fat milk in Tris-buffered saline (Biotopped) at room temperature for 1 h, the membrane was incubated at 4 °C for 12 h with rabbit monoclonal primary antibodies against MDR1 (1:1250; ab170904) and Anti-Sodium Potassium ATPase antibody-Plasma Membrane Loading Control (1:20,000; ab76020). Antibodies were both purchased from Abcam (Cambridge, United Kingdom). The membranes were incubated with horseradish peroxidase-conjugated AffiniPure Goat Anti-Rabbit IgG (ZSGB-BIO, Beijing, China) for 1 h and signals were observed using SuperSignal West Pico (Thermo Scientific, Waltham, MA). Western blotting bands intensity was quantified by densitometric analysis using Image J version 2 × (NIH Image Software, Bethesda, MA).

### ABC transporter-related ATPase activity assay

The activity of ABC transporter coupling ATPase was measured by monitoring the release of inorganic phosphate (Pi) from adenosine triphosphate (ATP) by ABC transporter membranes in the presence or absence of vanadate (Xia et al. 2007). Mice small intestine was homogenized with glass homogenizer (50 up/down strokes) to prepare membrane proteins using KenGEN Membrane and Plasma Protein Purification Kit (KenGEN BioTECH, Nanjing, China). Protein concentration was determined by using BCA Protein Quantitation Assay Kit (KenGEN BioTHCH, Nanjing, China). A 200 µL diluted membrane protein was pre-incubated in 200 µL inhibitor mix (4 mM ouabain, 4 mM EGTA, 10 mM NaN<sub>3</sub>, adjust to pH = 7). The ATPase reaction was measured in the presence or absence of 0.05 mM Na<sub>3</sub>VO<sub>4</sub> (vanadate) using Microscale Total ATPase Assay Kit (Nanjing Jiancheng Bloeng Inst., Nanjing, China) according to the instructions of the manufacturer. Briefly, 0.1 mL of the sample was pre-incubated in 0.42 mL assay buffer for 10 min at 37 °C. ATPase hydrolysis was accurately processed for 10 min by adding 0.1 mL of ATP stock solution, and then 100 µL of Reagent Four was immediately added to the mixture to end reaction. Mixture was centrifuged at 4000 rpm for 10 min and 0.3 mL of supernatant was transferred to 1 mL of chromogenic agent solution, incubated for 2 min at ambient temperature and the reaction was terminated with 1 mL of Reagent Six. The concentration of Pi was measured by the absorbance (A) at 636 nm wavelength and acquired by fitting in standard curve generated with series of Pi standard solution of varied concentrations.

### Statistical analysis

All data were analyzed using the SPSS 18.0 software (IBM, Armonk, NY). Data were indicated as mean ± SD. *T*-test obtained by one-way analysis of variance (ANOVA). *p* < 0.05 and *p* < 0.01 were considered to be statistically different.

## Results

### UHPLC-MS/MS analysis

Under optimized UHPLC conditions, ART and daidzein were eluted within 3.5 min as shown in Figure 3(B) and (C). In Figure 3(A), blank HBSS showed no interfering peaks at the retention times of each analyte. The calibration curve of ART was linear in

the concentration range of 3.91–2000.00 nM ( $y = 0.000412x + 0.00354$ ,  $r = 0.9932$ ,  $w = 1/x^2$ ). All coefficients of variation at each concentration are below 10%.

### Bidirectional transport assay in P-gp-over-expressing Caco-2 cell monolayers

Table 1 shows the permeability of ART across P-gp-over-expressing Caco-2 cell monolayers.  $P_{app}$  (AP-BL) values of ART from apical-to-basal side and  $P_{app}$  (BL-AP) from basal-to-apical side were  $2.40 \times 10^{-8}$  and  $3.54 \times 10^{-8}$  cm/s at 10 µM, respectively. For the ART-CHR combination group,  $P_{app}$  (AP-BL) and  $P_{app}$  (BL-AP) of ART became  $4.29 \times 10^{-8}$  (increased 1.79-fold) and  $2.85 \times 10^{-8}$  cm/s (decreased 1.24-fold), respectively. Efflux ratio ( $P_{BA}/P_{AB}$ ) in the ART-CHR combination group achieved 2.21-fold decrease ( $p < 0.01$ ) versus to ART alone. Thus ART has poor passive diffusion ability ( $P_{app} < 10^{-7}$  and efflux ratio < 2). Moreover, P-gp involved in ART efflux could be inhibited by CHR.

### MDR1 expression determined by RT-QPCR

As represented in Figure 4, ART alone significantly increased the level of MDR1 mRNA compared with the negative control ( $p < 0.05$ ). No significant difference was observed among negative and positive control or combined groups. When compared with ART alone, however, the MDR1 mRNA expressions in positive control (verapamil, ART-verapamil) and ART-CHR combined groups (1:0, 1:1, 1:2, 1:4, 0:1) were reversed to normal levels as well as negative control ( $p < 0.01$ ). CHR, therefore, could reverse the MDR1 up-regulated expression by ART. The lowest MDR1 mRNA level was obtained when the combined ratio of ART and CHR was 1:2. It suggested that binding sites of P-gp might be saturable.

### Determination of P-gp levels by western blot analysis

As shown in Figure 5(A) and (B), P-gp expression was up-regulated by ART alone ( $p < 0.05$ ) and verapamil ( $p < 0.05$ ). No significant difference was found among negative control and ART-verapamil or ART-CHR combined groups or CHR alone ( $p > 0.05$ ). Compared with ART alone, however, P-gp expression levels in ART-verapamil (1:1), ART-CHR (1:0.1, 1:1, 1:2, 1:4) and CHR alone significantly decreased ( $p < 0.05$  and  $p < 0.01$ ). In the presence and absence of CHR or verapamil, P-gp expression showed a significant difference. The results suggest that verapamil and CHR are capable of reversing ART-induced P-gp up-regulation.

### ABC transporter-related ATPase activity assay

Since ABC transporters are ATP-driven active transporters, ATPase activity is required to fuel the transportation activity. To test whether CHR influence the ABC transporter-related ATPase activity, microscale total ATPase assay kit was used to measure the ATPase activity. As shown in Figure 6, verapamil alone stimulates the ATPase activity ( $p < 0.05$ ) while ART alone remarkably decreased the ATPase activity versus the vehicle ( $p < 0.05$ ). When compared with ART alone, the ATPase activities determined in ART-CHR 1:4 and CHR alone groups achieved a slight increase ( $p < 0.05$ ).



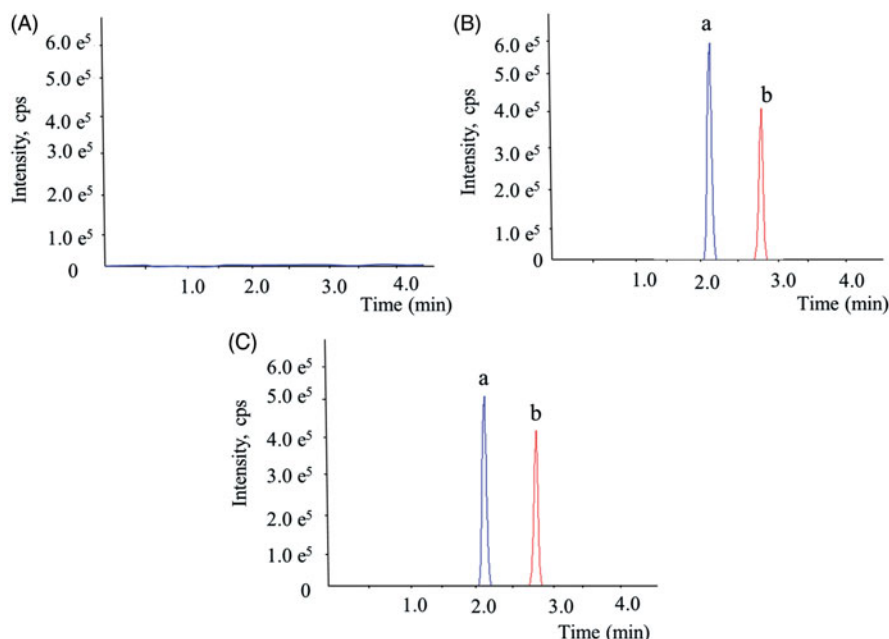


**Figure 3.** Representative full-scan chromatograms of (A) blank HBSS, (B) blank HBSS spiked with ART (a) and daidzein (b, IS) and (C) a study sample containing ART (a) and daidzein (b, IS) after incubation for 1 h.

**Table 1.** Permeability of ART across P-gp-over-expressing Caco-2 cell monolayers in the absence and the presence of CHR (mean  $\pm$  SD,  $n = 3$ ).

Drugs	Papp ( $\times 10^{-8}$ cm/s)		$P_{BA}/P_{AB}$ (efflux ratio)
	AP-BL	BL-AP	
ART (10 $\mu$ M)	2.40 $\pm$ 0.21	3.54 $\pm$ 0.27 <sup>##</sup>	1.48 $\pm$ 0.07
CHR-ART (2:1, 20:20 $\mu$ M)	4.29 $\pm$ 0.16 <sup>**</sup>	2.85 $\pm$ 0.04 <sup>##,*</sup>	0.67 $\pm$ 0.03 <sup>**</sup>

\* $p < 0.05$  and \*\* $p < 0.01$  versus ART; <sup>##</sup> $p < 0.01$  versus  $P_{app}$  (AP-BL).

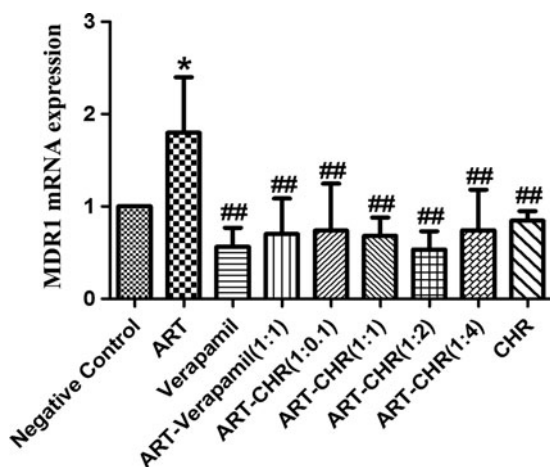


**Figure 4.** The expression of MDR1 mRNA in small intestine. MDR1 mRNA levels were determined by real-time qPCR after seven days oral xenobiotic pre-exposure in ICR mice. 0.5% CMC-Na was used as negative control and verapamil as positive control. All values were expressed as the mean  $\pm$  SD ( $n = 6$ ) for each group. \* $p < 0.05$  compared with negative control. # $p < 0.05$ , and ## $p < 0.01$  versus ART alone.

## Discussion

CHR belongs to the polymethoxylated flavonoids together with ART in the leaves and flowers of *A. annua*. The acetone layer of the industrial waste of ART is enriched with CHR. However, these industrial wastes are always discarded because few researchers focus on it. More recently, accumulating evidence suggested

that many flavonoids have the ability to inhibit CYP3A4 and P-gp activity (Sandor et al. 1998; Middleton et al. 2000; Daddam et al. 2014). Here, we have demonstrated that CHR exerts an inhibition not only on the rat CYP3A-mediated metabolism of ART as previously shown but also on its P-gp-mediated efflux through reversing the up-regulated P-gp and MDR1 expression levels induced by ART.

Interestingly, the lowest P-gp and MDR1 levels were both observed when the combination ratio between ART and CHR was 1:2. It is in accordance with our previous work (Wei et al. 2015). It was reported that the  $AUC_{0-t}$ ,  $C_{max}$ , and  $t_{1/2}$  of ART increased significantly as well as declined CL<sub>z</sub> after 3-d oral doses of ART in the presence of CHR (1:2) when compared with ART alone. Also, parasitaemia (%) remarkably attenuated 1.59-fold with 1.63-fold augmented inhibition (%) only when the ratio between ART and CHR reached 1:2. The results provided a direct proof that CHR in combination ratio of 1:2 with ART has a strong reversal effect on P-gp-mediated efflux of ART by down-regulating P-gp and MDR1 mRNA levels.

Verapamil, a classic substrate and inhibitor of P-gp, is a calcium channel blocker. It was reported that verapamil can increase the accumulation of Rh-123 in Caco-2 cells or MDCK-MDR1 (Chieli et al. 2012; Hu et al. 2016; Miao et al. 2016); therefore, it was always used as a reference compound to develop other P-gp substrates. Although verapamil inhibits P-gp function, several reports revealed that verapamil increased the P-gp level when it was applied alone (Collett et al. 2004; Grybauskas et al. 2015; Mohseni et al. 2016). Our results completely conform to the literatures. But recently, Miao et al. (2016) reported that verapamil down-regulated P-gp expression in Caco-2 cells. Therefore, the effect of verapamil on P-gp and MDR1 mRNA expression is still unclear.

P-gp is a member of the energy-dependent efflux pump associated with the excretion of many P-gp substrates and non-substrates, so ATPase activity plays an important role in the mechanisms of P-gp inhibition (Suri et al. 2008). As shown in Figure 6, ART inhibited the ATPase activity whereas verapamil significantly stimulated it. Our data are in consistent with the

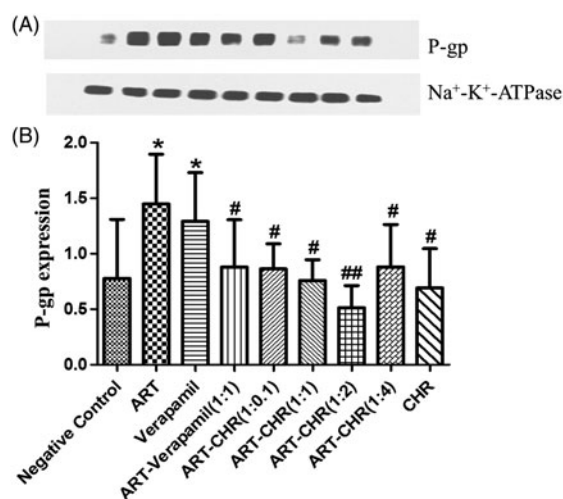


**Figure 5.** Impact of CHR on P-gp expression. (A) Western blot bands. (B) Quantification of P-gp assessed by Western blotting analysis was normalized to the expression level of  $\text{Na}^+\text{-K}^+\text{-ATPase}$  antibody. All values were expressed as the mean  $\pm$  SD ( $n=6$ ) for each group. \* $p < 0.05$  versus negative control. # $p < 0.05$  and ## $p < 0.01$  versus ART alone.

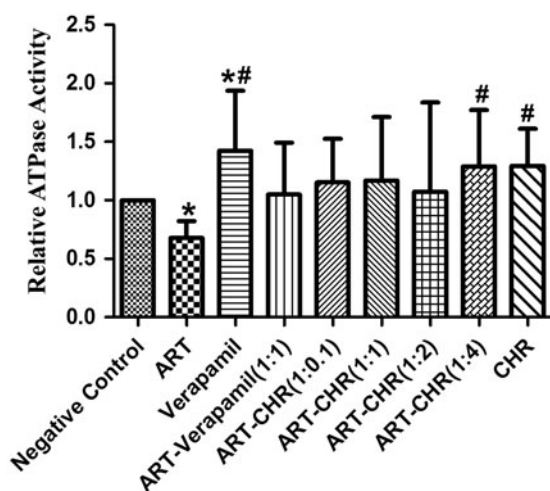


**Figure 6.** ABC transporter coupling ATPase activity in the mice small intestine. The impact of CHR in the absence and presence of ART on ATPase activity was investigated. \* $p < 0.05$  versus negative control. ## $p < 0.05$  versus ART alone.

results reported previously (Burk et al. 2005). CHR alone and ART-CHR in ratio of 1:4 had a slight stimulation on ATPase activity. Hence CHR as a P-gp inhibitor merely has a weak stimulating effect on ATPase activity.

In conclusion, CHR inhibits P-gp-mediated ART efflux through reversing MDR1 mRNA and P-gp up-regulated expression induced by ART and has very weak stimulation on ATPase activity. CHR, therefore, can be used as a promising P-gp small molecular inhibitor in the future. More importantly, the industrial waste of ART could be fully used to produce CHR: in fact it might be useful in reducing the cost of ART production.

### Acknowledgements

The authors are indebted to Dr. Ming Hu, Dr. Diana Chow and Mrs Taijun Yin from College of Pharmacology, University of Houston for

the bidirectional transport experiment in P-gp-over-expressing Caco-2 cell monolayers.

### Disclosure statement

The authors declare that they have no conflicts of interest concerning this article.

### Funding

This work was financially supported by the National Natural Science Foundation of China, 10.13039/501100001809 [81560580] Ningxia Nature Science Foundation [NZ14156].

### References

- Alcantara LM, Kim J, Moraes CB, Franco CH, Franzoi KD, Lee S, Freitas-Junior LH, Ayong LS. 2013. Chemosensitization potential of P-glycoprotein inhibitors in malaria parasites. *Exp Parasitol.* 134:235–243.
- Burk O, Arnold KA, Nussler AK, Schaeffeler E, Efimova E, Avery BA, Avery MA, Fromm MF, Eichelbaum M. 2005. Antimalarial artemisinin drugs induce cytochrome P450 and MDR1 expression by activation of xenosensors pregnane X receptor and constitutive androstane receptor. *Mol Pharmacol.* 67:1954–1965.
- Chen J, Li N, Wu XL, Liu C, Fan YR, Huang Y, Yu JQ, Bai CC, Han L, Fu XY, et al. 2014. \*The method to purify three polymethoxylated flavonoids from the industrial waste. China Patent no. ZL201210093926.0.
- Chieli E, Romiti N, Catiana Zampini I, Garrido G, Inés Isla M. 2012. Effects of *Zuccagnia punctata* extracts and their flavonoids on the function and expression of ABCB1/P-glycoprotein multidrug transporter. *J Ethnopharmacol.* 144:797–801.
- Collett A, Tanianis-Hughes J, Warhurst G. 2004. Rapid induction of P-glycoprotein expression by high permeability compounds in colonic cells *in vitro*: a possible source of transporter mediated drug interactions? *Biochem Pharmacol.* 68:783–790.
- Daddam JR, Dowlathabad MR, Panthangi S, Jasti P. 2014. Molecular docking and P-glycoprotein inhibitory activity of flavonoids. *Interdiscip Sci.* 6:167–175.
- Grybauskas A, Koga T, Kuprys PV, Nolan M, McCarty R, Walker L, Green KA, Norkett WM, Yue BY, Knepper PA. 2015. ABCB1 transporter and toll-like receptor 4 in trabecular meshwork cells. *Mol Vis.* 21:201–212.
- Hao S, Xiao Y, Lin Y, Mo ZT, Chen Y, Peng XF, Xiang CH, Li YQ, Li WN. 2016. Chlorogenic acid-enriched extract from *Eucommia ulmoides* leaves inhibits hepatic lipid accumulation through regulation of cholesterol metabolism in HepG2 cells. *Pharm Biol.* 54:251–259.
- Hu PY, Liu D, Zheng Q, Wu Q, Tang Y, Yang M. 2016. Elucidation of transport mechanism of paeoniflorin and the influence of ligustilide, senkyunolide I and senkyunolide A on paeoniflorin transport through Mdrk-Mdr1 cells as blood-brain barrier *in vitro* model. *Molecules.* 21:1–13.
- Inami M, Fukushima A, Ueno T, Yamada T, Tsunemi A, Matsumoto Y, Fukuda N, Soma M, Moriyama M. 2015. Reduction of dimethylnitrosamine-induced liver fibrosis by the novel gene regulator PI polyamide targeting transforming growth factor  $\beta$ 1 gene. *Biol Pharm Bull.* 38:1836–1842.
- Li Y, Revalde JL, Reid G, Paxton JW. 2010. Interactions of dietary phytochemicals with ABC transporters: possible implications for drug disposition and multidrug resistance in cancer. *Drug Metab Rev.* 42:590–611.
- Meng X, Liao S, Wang XY, Wang SX, Zhao XF, Jia P, Pei WJ, Zheng XP, Zheng XH. 2014. Reversing P-glycoprotein-mediated multidrug resistance *in vitro* by  $\alpha$ -asarone and  $\beta$ -asarone, bioactive *cis-trans* isomers from *Acorus tatarinowii*. *Biotechnol Lett.* 36:685–691.
- Meshnick SR, Taylor TE, Kamchonwongpaisan S. 1996. Artemisinin and the antimalarial endoperoxides: from herbal remedy to targeted chemotherapy. *Microbiol Rev.* 60:301–315.
- Miao Q, Wang ZY, Zhang YY, Miao PP, Zhao YY, Zhang YJ, Ma SC. 2016. *In vitro* potential modulation of baicalin and baicalein on P-glycoprotein activity and expression in Caco-2 cells and rat gut sacs. *Pharm Biol.* 25:1–9.
- Middleton E Jr, Kandaswami C, Theoharides TC. 2000. The effects of plant flavonoids on mammalian cells: implications for inflammation, heart disease, and cancer. *Pharmacol Rev.* 52:673–751.
- Mohseni M, Samadi N, Ghanbari P, Yousefi B, Tabasinezhad M, Sharifi S, Nazemiyeh H. 2016. Co-treatment by docetaxel and vinblastine breaks

- down P-glycoprotein mediated chemo-resistance. Iran J Basic Med Sci. 19:300–309.
- Nabekura T, Hiroi T, Kawasaki T, Uwai Y. 2015. Effects of natural nuclear factor-kappa B inhibitors on anticancer drug efflux transporter human P-glycoprotein. Biomed Pharmacother. 70:140–145.
- Numonov SR, Qureshi MN, Aisa HA. 2015. Development of HPLC protocol and simultaneous quantification of four free flavonoids from *Dracocephalum heterophyllum* Benth. Int J Anal Chem. 2015:1–5.
- Pal D, Kwatra D, Minocha M, Paturi DK, Budda B, Mitra AK. 2011. Efflux transporters- and cytochrome P-450-mediated interactions between drugs of abuse and antiretrovirals. Life Sci. 88:959–971.
- Sandor V, Fojo T, Bates SE. 1998. Future perspectives for the development of P-glycoprotein modulators. Drug Resist Update. 1:190–200.
- Sun RJ, Zeng M, Du T, Li L, Yang GY, Hu M, Gao S. 2015. Simultaneous determinations of 17 marker compounds in Xiao-Chai-Hu-Tang by LC-MS/MS: application to its pharmacokinetic studies in mice. J Chromatogr B Anal Technol Biomed Life Sci. 1003:12–21.
- Suri S, Taylor MA, Verity A, Tribolo S, Needs PW, Kroon PA, Hughes DA, Wilson VG. 2008. A comparative study of the effects of quercetin and its glucuronide and sulfate metabolites on human neutrophil function *in vitro*. Biochem Pharmacol. 76:645–653.
- Tripathi R, Rizvi A, Pandey SK, Dwivedi H, Saxena JK. 2013. Ketoconazole, a cytochrome P<sub>450</sub> inhibitor can potentiate the antimalarial action of  $\alpha/\beta$  arteether against MDR *Plasmodium yoelii* nigeriensis. Acta Trop. 126:150–155.
- Wang XM, Zhang X, Huang XH, Li YT, Wu MC, Liu JF. 2015. The drug–drug interaction of sorafenib mediated by P-glycoprotein and CYP3A4. Xenobiotica. 18:1–8.
- Wei SJ, Ji HY, Yang B, Ma LP, Bei ZC, Li X, Dang HW, Yang XY, Liu C, Wu XL, et al. 2015. Impact of chrysofenetin on the pharmacokinetics and anti-malarial efficacy of artemisinin against *Plasmodium berghei* as well as *in vitro* CYP450 enzymatic activities in rat liver microsome. Malar J. 14:1–13.
- Wesolowska O. 2011. Interaction of phenothiazines, stilbenes and flavonoids with multidrug resistance-associated transporters, P-glycoprotein and MRP1. Acta Biochim Pol. 58:433–448.
- White NJ. 2004. Antimalarial drug resistance. J Clin Invest. 113:1084–1092.
- Xia CQ, Milton MN, Gan LS. 2007. Evaluation of drug-transporter interactions using *in vitro* and *in vivo* models. Curr Drug Metab. 8:341–363.
- Yuan J, Wong IL, Jiang T, Wang SW, Liu T, Wen BJ, Chow LM, Wan Sheng B. 2012. Synthesis of methylated quercetin derivatives and their reversal activities on P-gp- and BCRP-mediated multidrug resistance tumour cells. Eur J Med Chem. 54:413–422.
- Zhang XW, Bu P, Liu L, Zhang XZ, Li J. 2015. Overexpression of long non-coding RNA PVT1 in gastric cancer cells promotes the development of multidrug resistance. Biochem Biophys Res Commun. 462:227–232.